

Sustainable Supercapacitor Electrode: The Role of Performance-Activated Carbon from *Nypa Fruticans* Shells

Muhammad Iqbal Al Fuady^{a,b*}, Ilmi Utari Simatupang^{a,b}, Putri Khoyrul Afifah^{a,b}

^aChemical Engineering Department, Vocational School, Universitas Sebelas Maret, Surakarta, Indonesia 57126

^bCenter of Excellence for Electrical Energy Storage Universitas Sebelas Maret, Surakarta, Indonesia 57126

*Corresponding author: miqbalalfuady@staff.uns.ac.id

DOI: <https://dx.doi.org/10.20961/equilibrium.v8i2.92471>

Article History

Received: 20-08-2024, Accepted: 02-01-2025, Published: 02-02-2025

Keywords:

Nypa Palm Shell,
Activated Carbon,
Electrode,
Supercapacitor.

ABSTRACT. Supercapacitors are energy storage devices widely used in electronics, representing a significant breakthrough in energy storage technology. Known as electric double-layer capacitors (EDLC), supercapacitors are electrochemical energy storage systems with higher power density than batteries. The material used to produce supercapacitor electrodes is waste from *Nypa* shells. The *Nypa* shells contain 36.5% cellulose, 21.8% hemicellulose, and 27.3% lignin. The production process uses the pyrolysis method to produce activated carbon, which is then used as supercapacitor electrode material. The SEM (Scanning Electron Microscope) test shows that all samples have different pore cavity structures in activated carbon. The EDX (Energy Dispersive X-ray) test shows that all activated carbon samples contain C, O, Mg, Si, and Ca elements. Based on FTIR (Fourier transform Infrared Spectroscopy) analysis, all samples had the same wave pattern, and functional groups in the form of O-H, C=C, C-H, and C≡C were detected. The BET test (Brunauer – Emmett – Teller) shows that activated carbon with C-NPS-Ox has a specific surface area, micropore surface area, total pore volume, and average pore diameter values of 989.3 m²/g, 537.1 m²/g, 56.5 cm³/g, and 11.4 nm. The CV (Cyclic Voltammetry) test shows that the C-NPS-Ox sample with a scan rate of 10 mV/s has the highest specific capacitance value, 142.44 F/g. With the large capacity obtained, C-NPS-Ox has the potential to be used as a supercapacitor material.

1. INTRODUCTION

In recent years, the development of renewable and sustainable energy has been identified as an effective strategy to address the crises of environmental pollution and climate change. With increasing demand, many renewable energy sources have become scarce and cannot be used consistently, except for conversion into electricity [1]. To tackle this issue, the development of high-performance, low-cost, and, most importantly, environmentally friendly energy storage devices are necessary, such as lithium-ion batteries, supercapacitors, and Zn-air batteries. As one form of renewable energy storage, supercapacitors promise innovative products with reliable lifecycles, excellent power density, ultra-fast charging rates, and a wide range of operating conditions [2]. Supercapacitors are energy storage devices widely used in electronics and represent a breakthrough in energy storage technology. Known as EDLCs (Electric double-layer capacitors), supercapacitors have many advantages over batteries, including a higher power density (>10 kW/kg), rapid charging and discharging capabilities with high stability, a long charge cycle life (>10⁶ cycles), and an energy density that can be 10⁶ to 10⁹ times greater than that of conventional capacitors [3].

Activated carbon has the potential to be utilized as a supercapacitor electrode material due to its high energy density, affordability, abundant raw material availability, and pore size within the micropore-mesopore range (2–50 nm) [4]. The large surface area facilitates the formation of a multilayer electric field on the electrode surface [5]. Activated carbon can be produced from organic and inorganic materials, provided the raw material has a porous structure. Biomass can serve as a raw material for making activated carbon because it is composed of lignocellulose, cellulose, and hemicellulose, which are organic carbon sources. Examples of biomass that can be utilized include coal, coconut shells, palm kernel shells, pine waste, wood waste, and others [6].

This study utilized biomass in the form of *Nypa* palm shell waste as a raw material for the production of

activated carbon because the distribution of Nypa trees reaches 231 hectares and produces Nypa fruit, amounting to 36 tons per year. With the amount of Nypa fruit produced, the Indonesian community has only utilized the flesh of the Nypa fruit to create processed food products such as candies. At the same time, the skin, especially the shell, is often overlooked as it is considered waste and not utilized. [7]. The waste produced by Nypa palm shells reaches 1.01 tons per year [8].

Based on the content of the nypa palm shells, nypa palm shells produce cellulose content of 36.5%, hemicellulose of 21.8%, and lignin of 27.3% [9]. The presence of lignin means that the activated carbon produced from Nypa palm shell waste contains a high amount of carbon. The high cellulose content also allows for consistent and even combustion, resulting in good-quality carbon that can serve as raw material for producing activated carbon for supercapacitor electrodes.

In this study, pyrolysis methods will repurpose Nypa palm shell waste into activated carbon. Pyrolysis is the best and most sustainable choice for protecting the environment while enhancing the quality of activated carbon. By analyzing the potential use of Nypa palm shell waste as a material for producing electrodes in supercapacitors using activated carbon, it is hoped that the added value of this waste can be increased and its utilization optimized.

2. MATERIALS AND METHODS

The materials used in this research include Nypa palm shell waste, potassium hydroxide (KOH) (Merck), sulfuric acid (H_2SO_4) 95-97% (Merck), aquadest (Onemed), filter paper, acetylene black (AB) (Denka), polyvinylidene fluoride (PVDF) (Arkema/Solvay), n-methyl pyrrolidinone (NMP) (Merck), nickel plate, carbon dioxide gas (CO_2), and nitrogen gas (N_2).

The tools used in this research include a grinding machine (Aosenr), muffle furnace (Nabertherm), electric stove (IKA C-MAG HS 7), oven, analytical scales (Ohaus NVT6201), stirring motor (OEM), mortar and pestle, Erlenmeyer beaker (Pyrex), glass funnel (Pyrex), spoon, glass stirrer, porcelain cup (Pyrex), measuring cup (Pyrex), universal indicator (Mquant), measuring pipettes (Pyrex), pump pipettes, and thermometers (Gea). In this research, several instruments were used, including SEM-EDX (Jeol-JCM 7000), BET (Quantachrome NovaWin), FTIR (IR Spirid Shimadzu), and CV (Potentiostat EZstat Pro).

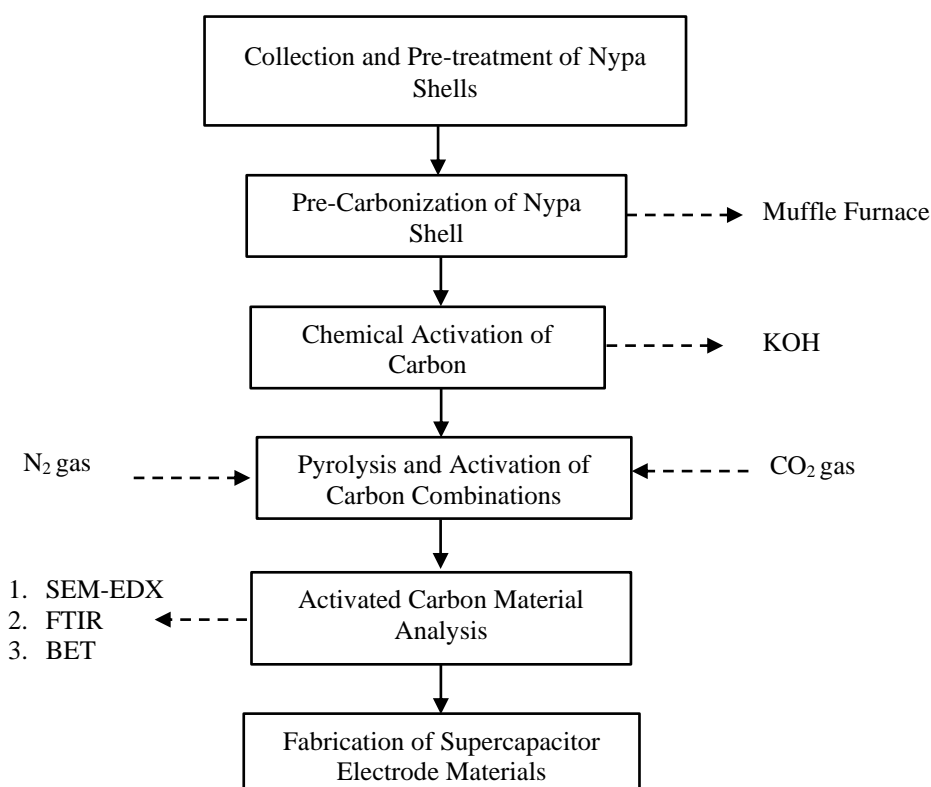


Figure 1. Flow Chart of Producing Activated Carbon From Nypa Palm Shells

2.1. Preparation of Activated Carbon Nypa Palm Shells

The production of activated carbon from Nypa palm shell waste as a supercapacitor electrode material involves several stages: collection and pre-treatment of the Nypa palm shell, pre-carbonization of the Nypa palm shell using a muffle furnace, chemical activation of the carbon with KOH solution, carbon pyrolysis in a muffle furnace with N₂ gas flow, and a combination activation (physical & chemical) of the carbon using a muffle furnace with CO₂ gas flow. The process begins with collecting Nypa palm waste from disposal sites of Nypa plantations, which is then separated into shells and fiber using a machete. The Nypa palm shell is sun-dried for 3–4 days until completely dry. Once dried, the Nypa palm shell is reduced in size using a grinding machine with a mesh size of 50. The ground Nypa palm shell then proceeds to the pre-carbonization stage. This phase involves heating the shell at 200°C for 1 hour in a muffle furnace. The pre-carbonization process at 200°C causes the Nypa palm shell to transform into a black carbon material gradually. The carbon obtained from pre-carbonization is ground finer using a mortar and pestle, followed by sieving with a 200 mesh sieve to maximize the chemical activation process.

In this study, two variations were conducted during the process of making activated carbon. The first variation was activated carbon from a Nypa palm shell that went through a chemical activation stage (C-NPS-Ox). In this variation, the carbon is processed by mixing the carbon in an 80°C KOH solution (carbon: KOH solution ratio of 1:6.7), accompanied by stirring at 450 rpm for 1 hour [10], with a 3M concentration of KOH used in this activation stage. After completion, the carbon is filtered using filter paper and dried in an oven at 100°C for 24 hours. In the second variation, the activated carbon from the Nypa palm shell did not go through a chemical activation stage (C-NPS). Both variations of the activated carbon then underwent pyrolysis in a muffle furnace at a temperature of 600°C for 1 hour, with a nitrogen gas flow. The pyrolyzed carbon is subsequently re-activated using a combination of physical and chemical methods in a muffle furnace at a temperature of 800°C for 1 hour, with a carbon dioxide gas flow [10]. The activated carbon obtained from the subsequent activation combination is washed with distilled water until a neutral pH is achieved and then dried in an oven at 100°C for 24 hours. The dried activated carbon is then finely ground and sieved using a 500 mesh sieve.

2.2. Fabrication of Supercapacitor Electrode Materials

The activated carbon made is then added as the conductive material acetylene black (AB) and the binding material (binder) in the form of polyvinylidene fluoride. (PVDF). The ratio of activated carbon: AB: PVDF is 8: 1: 1 [11]. In this research, the activated carbon used was 8 grams, AB 1 gram, and PVDF 1 gram.

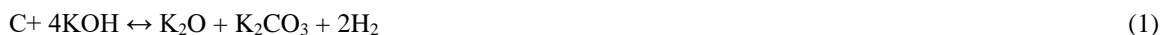
All ingredients are mixed with the addition of n-methyl pyrrolidone (NMP) little by little until an electrode slurry is formed and layered on an aluminum plate with a thickness of 200 microns. Next, the plate that has been coated is dried in a vacuum oven at 100°C for 1 hour.

2.3. Characterization of Activated Carbon and Supercapacitor Electrode Materials

The activated carbon produced, with varying concentrations of KOH activator at 3M and without an activator, is further tested using SEM-EDX, BET, and FTIR analyses, while the performance of the resulting supercapacitor electrodes is evaluated through Cyclic Voltammetry.

3. RESULTS AND DISCUSSION

Producing activated carbon from Nypa palm shell waste has several stages: collection and pre-treatment of Nypa palm shells, pre-carbonization, chemical activation, pyrolysis, and combination activation (physics & chemical). The chemical reactions that occur during the activation process are as follows:



In this reaction, the free carbon in the Nypa palm shell bonds with KOH to form a carbonate compound (K₂CO₃), as evidenced by the discovery of a small amount of white powder-like ash in the activated carbon resulting from chemical activation. These bonds make carbon have holes called pores. The more free carbon that is bound, the carbon will have many pores with a large surface area. KOH is a dehydrating agent, so a dehydration reaction occurs upon chemical activation. The dehydration reaction will erode the carbon and increase the surface

area of the activated carbon due to the formation of more pores. This reaction also helps to improve the efficiency of the activated carbon activation process [12].

3.1 Scanning Electron Microscope (SEM) Test Analysis

Scanning Electron Microscope (SEM) testing was conducted to determine the morphology and particle size. Identification of the particle morphology of a material can be done at various magnifications. The image magnification taken in this test is 2,500x magnification. The results of the SEM analysis of activated carbon of Nypa palm shells from this research are shown in Figure 2 below:

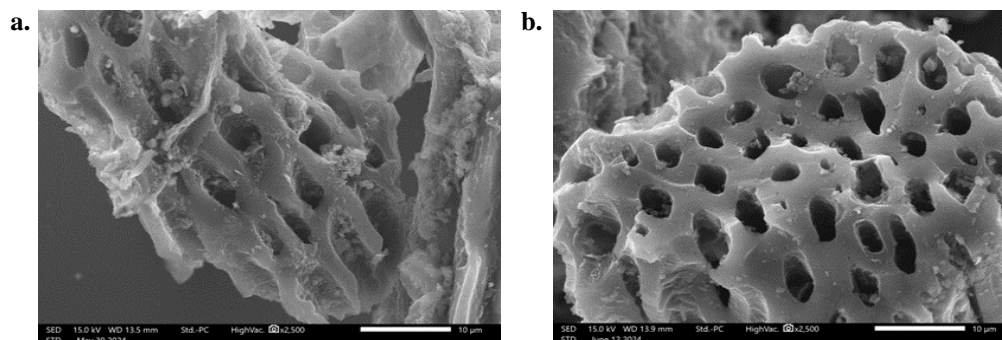


Figure 2. (a) Morphology of Porous Carbon Synthesized From Nypa Palm Shell Activated Without KOH (C-NPS) (b) After Activation With KOH (C-NPS-Ox)

Based on Figure. 2, the difference in the structure of the pore cavity in activated carbon. In Figure (a), activated carbon without KOH (C-NPS) shows that the carbon has few large pore cavities, somewhat elongated in shape, still accompanied by partitions between the pore cavities, and there are impurities around the pore cavities. Meanwhile, in Figure (b), activated carbon with KOH (C-NPS-Ox) shows that the pore cavities are more evenly distributed, with smaller sizes but larger volumes, no partitions between the pore cavities, and significantly fewer impurities.

3.2 Energy Dispersive X-Ray (EDX) Test Analysis

Energy Dispersive X-ray (EDX) is used to determine the chemical element content of a material. This test produces an energy spectrum that reflects the presence and intensity of each element in the sample, thus providing more accurate information that can support the image resulting from morphological analysis using SEM. Analysis using EDX obtained results in percentages of active carbon elements, which can be seen in Figure. 3 and Table 1.

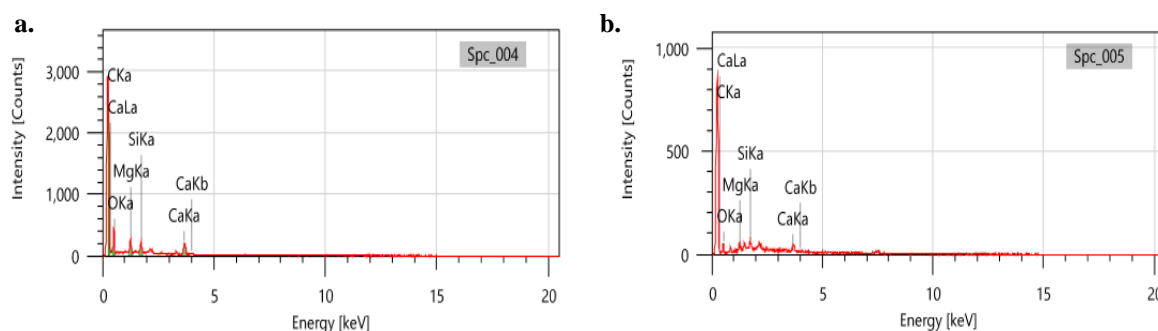


Figure 3. Sample Element Content Analysis Graph using EDX (a) Activated without KOH (C-NPS) (b) After Activation with KOH (C-NPS-Ox)

Table 1. Analysis of Active Carbon Material Composition from EDX Results

Element	Activator Concentration			
	C-NPS		C-NPS-Ox	
	Mass (%)	Atoms (%)	Mass (%)	Atoms (%)
C	55.18	65.21	67.45	76.63
O	33.42	29.65	22.30	19.02
Mg	3.37	1.97	2.44	1.37
Si	2.16	1.09	2.29	1.11
Ca	5.87	2.08	5.51	1.88

Table 1 shows that the most abundant composition contained in active carbon from Nypa palm shells is the element carbon (C). The high C content indicates that the activated carbon sample has high purity. The element oxygen (O) has the second highest percentage after element C, which is indicated by the oxygen content in the carbon sample during pyrolysis not being completely decomposed or bonds occurring during the activation process. The elements silica (Si) and magnesium (Mg) were identified in active carbon because these two elements are macronutrients in palm shells that play an important role in photosynthesis. The calcium (Ca) content in activated carbon is caused by the chemical content in Nypa palm shells, one of which is Ca [9].

During the activation process, silica, magnesium, and calcium have high stability, so they do not react easily and decompose completely at pyrolysis and activation temperatures, causing these elements to become impurities and affecting the adsorption effectiveness of activated carbon.

The presence of the carbon element C with the highest mass and atomic proportions indicates the potential for high adsorption capacity on the sample. The wide pore structure will provide a large surface for interaction with molecules or ions. For example, the pores identified as micropores and mesopores in activated carbon provide a large surface area to adsorb ions in supercapacitors, thereby increasing the energy storage capacity [13].

On the other hand, a high oxygen content indicates the presence of oxygen functional groups on the carbon surface. The oxygen element group (O) functions to increase surface wettability and capacitance values, which play an important role in electrolyte penetration and electrochemical performance in supercapacitor electrodes [13].

3.3 Fourier transform Infrared Spectroscopy (FTIR) Test Analysis

Analysis of activated carbon functional groups was carried out using Fourier transform Infrared Spectroscopy (FTIR) IR Spirid Shimadzu tool. The results obtained can be seen in Figure 4 below:

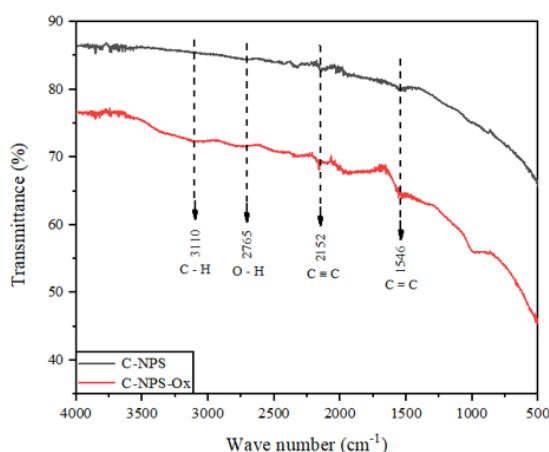
**Figure 4.** Results of Functional Group Analysis of Activated Carbon using FTIR

Figure. 4 shows that all samples show very similar spectral shapes. At wave number 1536 - 1680 cm^{-1} , the aromatic C=C functional group is formed; shown at wave number 1546 cm^{-1} , there is an increase in the active carbon absorption area. This indicates that the activated carbon obtained is purer after the chemical activation process so that the resulting value is greater [9]. Apart from that, wave number 2891-2622 cm^{-1} shows that the O-

H functional group appears after carbon has been activated chemically and physically, indicating the presence of oxygen [14]. The presence of oxygen can increase the wettability of electrode materials in aqueous electrolytes and increase capacitance through Faradaic reactions [15]. However, it can also affect the resistivity of activated carbon, which is a barrier to electron transfer [16].

The wave numbers 3300 - 3100 cm^{-1} indicate that the C-H functional group in activated carbon undergoes hydrogenation during the activation process [9]. Additionally, wave numbers 2260 - 2100 cm^{-1} show the $\text{C} \equiv \text{C}$ alkyne functional group, specifically at wave number 2152 cm^{-1} . This indicates that pure activated carbon is produced through the carbonization process, thereby enhancing its conductivity properties [9]. From the functional groups detected, it can be seen that all samples form the same spectrum and provide good properties for the active carbon material. The functional group grouping is dominated by O-H, C=C, C-H, and $\text{C} \equiv \text{C}$.

3.4 Brunauer-Emmett-Teller Test Analysis

The Brunauer-Emmett-Teller (BET) test is carried out to quantitatively determine the characteristics of a material, including specific surface area, total number of pores, total pore volume, and average pore diameter. This test uses the Nova Station A tool, which works on two principles: degassing and analyzing. The *degassing* process was carried out at a temperature of 300°C and flowed with N_2 gas for 2 hours, with the aim of removing molecules adsorbed on the surface of the material, opening pores on the surface, and increasing the ability to interact with molecules or ions [17]. The BET test results are displayed in Table 2.

Table 2. Characteristics of Activated Carbon from BET Testing Results

Parameter	C-NPS	C-NPS-Ox
Specific surface area (m^2/g)	634.7	989.3
Micropore surface area (m^2/g)	393.2	537.1
Total pore volume (cm^3/g)	34.9	56.5
Average pore diameter (nm)	11.0	11.4

Based on the data displayed in Table 2, it is shown that C-NPS-Ox has a specific surface area of 989.3 m^2/g . This figure is higher compared to the specific surface area of C-NPS, which is 634.7 m^2/g . The specific surface area, micropore surface area, and total pore volume of C-NPS-Ox have higher values than C-NPS. This proves that using KOH in chemical activation effectively increases the surface area and volume of activated carbon.

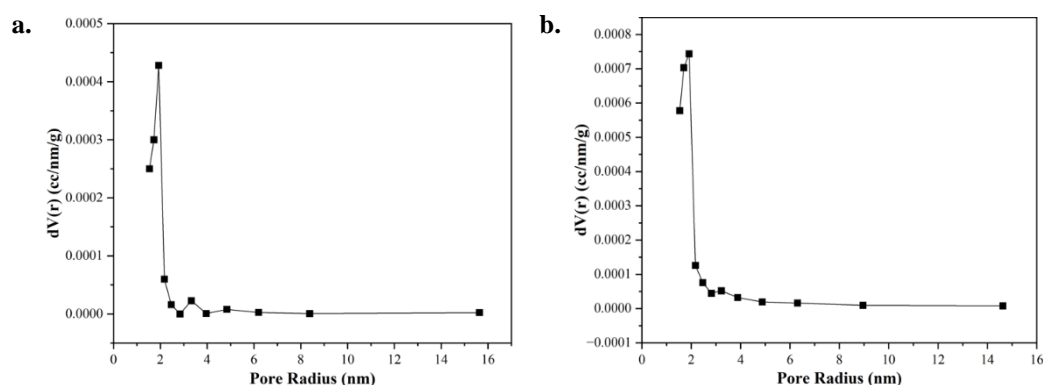


Figure 5. BJH Desorption Graph (a) Activated Without KOH (C-NPS) (b) After Activation With KOH (C-NPS-Ox)

The BET test results also show that C-NPS and C-NPS-Ox have an average pore diameter of 11.0 nm and 11.4 nm, respectively. This large diameter is classified as mesoporous size activated carbon, namely active carbon whose diameter is between 2 nm and 50 nm. Mesoporous carbon is very suitable for use in supercapacitor electrodes because mesoporous carbon has a large surface area, allowing more electrolyte ions to interact with the electrode surface. Mesopores function as ion transport pathways for energy storage. Meanwhile, micropores have a pore size of < 2 nm, which acts as an ion reservoir for energy storage. In addition, good conductivity in electron transfer accelerates the rate of electrochemical reactions and improves the performance of supercapacitors. The

stable structure of mesoporous carbon also makes it resistant to degradation during charge and discharge cycles [4].

A factor that influences the quality of porous carbon apart from its surface area is the uniformity of pore size distribution. The more uniform the pore size distribution of a carbon, the more uniform the pore size of the carbon will be. To describe the pore size distribution of a material, you can use the Barrett, Joyner, and Halenda (BJH) desorption method. The pore structure of activated carbon has a pore size distribution consisting of micropores (< 2.0 nm), mesopores (2 - 50 nm), and macro pores (> 50 nm) [18]. Figure 5. shows the pore size distribution for activated carbon without KOH (C-NPS) and after activation with KOH (C-NPS-Ox).

From Figure 5, it can be seen that the pore distribution of C-NPS carbon ranges from 1.5 nm to 15.6 nm. In contrast, the pore distribution ranges from 1.5 nm to 14.6 nm for C-NPS-Ox activated carbon. C-NPS has a wider range of pores because C-NPS does not undergo a chemical activation stage. The chemical activation process leads to an increase in the number of micropores (small-sized pores) and a more uniform pore distribution, thereby increasing the specific surface area. The pore formation in C-NPS is influenced only by the pyrolysis process without aggressive chemical treatment, resulting in a tendency to retain macropores or mesopores (larger-sized pores), which causes it to have a larger pore radius and lower surface area compared to chemically activated carbon (C-NPS-Ox).

3.5 Cyclic Voltammetry (CV) Test Analysis

The electrochemical performance test used cyclic voltammetry with a Potentiostat EZstat Pro. This method measures the properties of an electrochemical cell, such as potential, capacitance, and cycle life. The test uses three electrodes: reference (Ag/AgCl), counter (platinum), and working (Nypa palm shell activated carbon). The supercapacitor samples consist of variations C-NPS and C-NPS-Ox. The electrolyte solution used is 1M H₂SO₄.

The use of acidic electrolytes such as H₂SO₄ can increase ionic conductivity, as shown in Farma's (2021) research on making supercapacitors based on nypa fruit husk. This study shows that the use of H₂SO₄ solution as a supercapacitor electrolyte solution produces a specific capacitance value of 214.31 F/g, higher than that of KOH, which only produces 173.43 F/g [19]. This proves that the performance of the H₂SO₄ electrolyte is higher than that of the KOH solution. This proves that the performance of the H₂SO₄ electrolyte is more optimal than the alkaline electrolyte. The voltage applied to the working electrode samples is 0 V to 1 V. Figure 6. The test results are in the form of CV graphs with scan rate variations of activated carbon without KOH (C-NPS) and after activation with KOH (C-NPS-Ox).

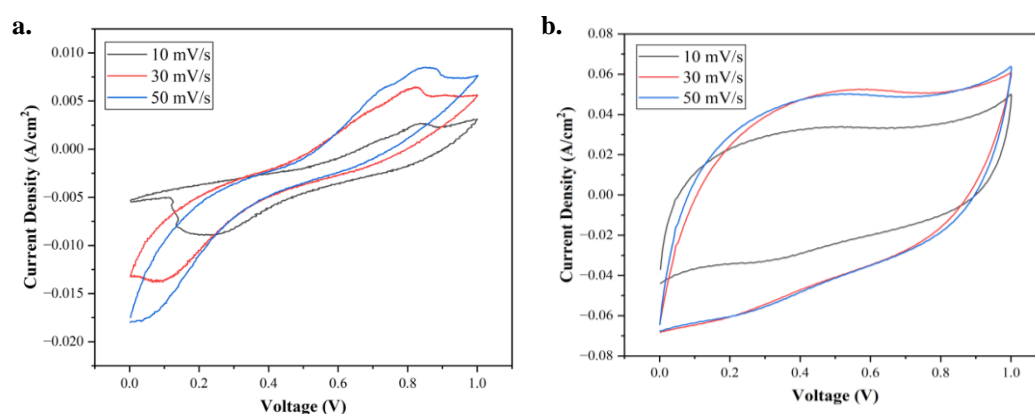


Figure 6. CV Curve of Nickel Plate with Scan Rate Variations (a) Activated without KOH (C-NPS) (b) After Activation with KOH (C-NPS-Ox)

Figure. 6 shows that activating activated carbon with KOH affects the increase in the area formed in the CV graph. C-NPS-Ox produces the curve with the largest area compared to C-NPS. This is evident from the shape of the curve, which is closer to a rectangle. A curve that approaches a rectangular shape indicates that the electrode has good capacitive behavior and normal EDLC properties [20].

The widening CV curve makes it difficult to maintain a quasi-rectangular shape because there is less time available for ions to move from the electrolyte to the electrode surface [9]. Through the formed curve image, the

area calculation can be determined with the help of OriginLab software. The area data will be used to calculate the specific capacitance value produced by the Nypa palm shell-activated carbon electrode for each variation. Based on Table 3, the Specific Capacitance Data of Electrodes with Nickel Plates of activated carbon without KOH (C-NPS) and after activation with KOH (C-NPS-Ox) are compared.

Table 3. Specific Capacitance Data of Electrodes with Nickel Plates

Sample	Scan Rate (mV/s)	Specific Capacitance (F/g)
C-NPS-Ox	10	142.44
	30	67.56
	50	47.22
C-NPS	10	7.26
	30	3.32
	50	2.06

Table 3 shows that the highest specific capacitance value is found in C-NPS-Ox at a scan rate of 10 mV/s, which is 142.44 F/g. From Table 3, it can also be seen that the capacitance value decreases with each increase in scan rate. This is because the resistivity increases at higher scan rates, reducing the ability to conduct electricity. Additionally, the low capacitance at high scan rates is due to the fact that ions require a longer time to diffuse into the pores of the carbon electrode; at high scan rates, the ions only reach the surface of the carbon [19].

In the study conducted by Farma (2021) on the development of supercapacitors using nipa palm fruit husk as the base material, a capacitance value of 214.31 F/g was obtained [19]. This capacitance value is higher compared to the results of this study, indicating that further research is needed to identify the factors influencing the capacitance value and ways to enhance the capacitance of supercapacitors made from Nypa palm shells. Further research can be conducted by increasing the concentration of KOH during the chemical activation process, as this study only used 3M KOH.

4. CONCLUSION

Nypa palm shell waste can be used as supercapacitor electrode material as activated carbon made by the pyrolysis method. From the results of SEM-EDX, FTIR, BET, and CV tests, it can be concluded that the KOH activator effectively improves the quality of activated carbon from the Nypa palm shell. The SEM test shows that the C-NPS-Ox has a significantly higher number of pores with larger volume, without barriers, and fewer impurities. The EDX test results indicate that the C-NPS-Ox carbon content is higher than the C-NPS. The BET test results show that the C-NPS-Ox has a much larger surface area of 989.3 m²/g. Electrochemical tests by CV testing showed the best results on electrode samples with C-NPS-Ox. The specific capacitance value obtained was 142.44 F/g. The use of the KOH activator and the smaller the scan rate used, the greater the specific capacitance produced in the supercapacitor.

ACKNOWLEDGEMENTS

The authors acknowledge the financial support from Lembaga Penelitian dan Pengabdian Masyarakat Universitas Sebelas Maret (LPPM-UNS) through Penelitian Hibah Grup Riset (HGR) Scheme with contract number 194.2/UN27.22/PT.01.03/2024. We also thank the Center of Excellence for Electrical Energy Storage Technology at Universitas Sebelas Maret for providing research facilities.

REFERENCES

- [1] L. Luo *et al.*, "High performance supercapacitor electrodes based on B/N Co-doped biomass porous carbon materials by KOH activation and hydrothermal treatment," *Int. J. Hydrogen Energy*, vol. 46, no. 63, pp. 31927–31937, 2021, doi: 10.1016/j.ijhydene.2021.06.211.
- [2] L. Luo *et al.*, "A review on biomass-derived activated carbon as electrode materials for energy storage supercapacitors," *J. Energy Storage*, vol. 55, no. PD, p. 105839, 2022, doi: 10.1016/j.est.2022.105839.
- [3] A. Nurul Huda, "Pemanfaatan Karbon Aktif dari Sekam Padi Sebagai Elektroda Superkapasitor," *J. Ilmu dan Inov. Fis.*, vol. 6, no. 2, pp. 102–113, 2022, doi: 10.24198/jiif.v6i2.39639.
- [4] T. Ariyanto, I. Prasetyo, and R. Rochmadi, "Pengaruh Struktur Pori Terhadap Kapasitansi Elektroda Superkapasitor Yang Dibuat Dari Karbon Nanopori," *Reaktor*, vol. 14, no. 1, 2012, doi:

- 10.14710/reaktor.14.1.25-32.
- [5] O. N. Tetra, “Superkapasitor Berbahan Dasar Karbon Aktif Dan Larutan Ionik Sebagai Elektrolit,” *J. Zarah*, vol. 6, no. 1, pp. 39–46, 2018, doi: 10.31629/zarah.v6i1.293.
- [6] S. Haryati, A. T. Yulhan, and L. Asparia, “Pembuatan Karbon Aktif Dari Kulit Kayu Gelam (*Melaleuca leucadendron*) yang Berasal Dari Tanjung Api-Api Sumatera Selatan,” *J. Tek. Kim. Fak. Tek. Univ. Sriwij.*, vol. 23, no. 2, pp. 77–86, 2017.
- [7] D. R. Gusti, U. Lestari, I. Lestari, and I. L. Tarigan, “Pemanfaatan Limbah Cangkang Buah Nipah Menjadi Masker Gel Peel Off Pada Ibu-Ibu PKK Kelurahan Kampung Laut Tanjung Jabung Timur,” *J. Karya Abdi Masy.*, vol. 4, no. 3, pp. 630–636, 2021, doi: 10.22437/jkam.v4i3.11587.
- [8] N. M. Heriyanto, E. Subiandono, and E. Karlina, “POTENSI DAN SEBARAN NIPAH (*Nypa fruticans* (Thunb.) Wurmb) SEBAGAI SUMBERDAYA PANGAN,” *J. Penelit. Hutan dan Konserv. Alam*, vol. 8, no. 4, pp. 327–335, 2011, doi: 10.20886/jphka.2011.8.4.327-335.
- [9] R. Farma *et al.*, “Enhanced electrochemical performance of oxygen, nitrogen, and sulfur doped Nypa fruticans-based carbon nanofiber for high performance supercapacitors,” *J. Energy Storage*, vol. 67, no. April, 2023, doi: 10.1016/j.est.2023.107611.
- [10] R. Farma, V. Asyana, and I. Apriyani, “Activation of nipah fruit coir-derived carbon material with KOH and NH₃ for supercapacitor cell applications,” *J. Aceh Phys. Soc.*, vol. 11, no. 4, pp. 115–120, 2022, doi: 10.24815/jacps.v11i4.28601.
- [11] S. U. Muzayana, C. S. Yudha, L. M. Hasanah, A. Nur, and A. Purwanto, “PENGARUH PEMANASAN PADA PROSES PRETREATMENT UNTUK DAUR ULANG MATERIAL KATODA BATERAI LI-ION Effect of Heating on the Pretreatment Process for Recycling Li-Ion Battery Cathode,” vol. 4, no. 2, pp. 105–114, 2019.
- [12] I. Susanti and N. Widiastuti, “Activation of zeolite-Y templated carbon with KOH to enhance the CO₂ adsorption capacity,” *Malaysian J. Fundam. Appl. Sci.*, vol. 15, no. 2, pp. 249–253, 2019, doi: 10.11113/mjfas.v15n2.914.
- [13] R. Farma *et al.*, “Jurnal Penyimpanan Energi sulfurNypa buah-buahanserat nano karbon berbasis untuk superkapasitor berkinerja tinggi,” vol. 67, no. April, 2023.
- [14] R. D. Asti and A. Putra, “Pengaruh Jenis Larutan Elektrolit Terhadap Sifat Elektrokimia Superkapasitor dari Karbon Aktif Sabut Kelapa Program Studi Kimia , Universitas Negeri Padang,” vol. 8, pp. 19496–19504, 2024.
- [15] S. Xin *et al.*, “Chemical structure evolution of char during the pyrolysis of cellulose,” *J. Anal. Appl. Pyrolysis*, vol. 116, pp. 263–271, 2015, doi: 10.1016/j.jaap.2015.09.002.
- [16] A. G. Pandolfo and A. F. Hollenkamp, “Carbon properties and their role in supercapacitors,” *J. Power Sources*, vol. 157, no. 1, pp. 11–27, 2006, doi: 10.1016/j.jpowsour.2006.02.065.
- [17] Y. Hidayat, I. Nurcahyo, F. Rahmawati, K. Dwi N, and W. W. Lestari, “Penambahan Karakter Luas Permukaan Dan Ukuran Pori Arang Sebagai Upaya Diversifikasi Produk Arang Dari Tempurung Kelapa Pada Cv. Solo Button,” *J. Kewirausahaan dan Bisnis*, vol. 24, no. 14, p. 94, 2019, doi: 10.20961/jkb.v24i14.37724.
- [18] A. Imammuddin, S. Soeparman, W. Suprpto, and A. Sonief, “Pengaruh Temperatur Karbonisasi terhadap Mikrostruktur dan Pembentukan Kristal pada Biokarbon Eceng Gondok sebagai Bahan Dasar Absorber Gelombang Elektromagnetik Radar,” *J. Rekayasa Mesin*, vol. 9, no. 2, pp. 135–141, 2018, doi: 10.21776/ub.jrm.2018.009.02.10.
- [19] R. Farma, A. N. I. Lestari, and I. Apriyani, “Supercapacitor cell electrodes derived from Nipah Fruticans fruit coir biomass for energy storage applications using acidic and basic electrolytes,” *J. Phys. Conf. Ser.*, vol. 2049, no. 1, 2021, doi: 10.1088/1742-6596/2049/1/012043.
- [20] K. Scott, *Electrochemical Principles and Characterization of Bioelectrochemical Systems*. Elsevier Ltd., 2016. doi: 10.1016/B978-1-78242-375-1.00002-2.